

The cytopathic 18f strain of *Hepatitis A virus* induces RNA degradation in FrhK4 cells

**M. Kulka, A. Chen, D. Ngo, S. S. Bhattacharya,
T. A. Cebula, and B. B. Goswami**

Food and Drug Administration, Center for Food Safety and Applied Nutrition,
Division of Molecular Biology, Laurel, MD, U.S.A.

Received November 13, 2002; accepted March 10, 2003
Published online June 2, 2003 © Springer-Verlag 2003

Summary. The mechanism responsible for the induction of apoptosis by the rapidly replicating HM175/18f strain of *Hepatitis A virus* (HAV) was investigated. Full length HAV RNA and viral capsid protein VP1 were detected in 18f infected cells at earlier times post-infection than in HM175/clone 1 infected cells. Analysis of total cellular RNA from HM175/18f infected FrhK4 cells by denaturing agarose gel electrophoresis and Northern blot hybridization revealed extensive degradation of both the 28S and 18S ribosomal RNA (rRNA) molecules. Similar degradation was observed when these cells were infected with *Human coxsackievirus* B1, a fast replicating enterovirus. In contrast, the parental strain of 18f, HM175/clone 1 did not induce RNA degradation. Inhibition of RNA degradation correlated with inhibition of virus replication. The pattern of rRNA degradation resembled degradation of rRNAs by RNase L, an enzyme activated in interferon-treated cells following infection with certain viruses. Ribosomal RNA degradation was accompanied by the reduction in the levels of several cellular RNAs including those for β -actin and glyceraldehyde-3-phosphate dehydrogenase, while the levels of c-myc and c-jun were higher. Interferon mRNAs could not be detected in either infected or mock-infected control cells, and STAT1, a key regulator of interferon action was not phosphorylated following virus infection. These results reveal a heretofore-undescribed pathway that involves the regulation of RNA degradation and apoptosis following HAV/18f replication in FrhK4 cells.

Introduction

Hepatitis A virus (HAV), the only member of the genus *Hepatovirus* within the *Picornaviridae* family, is a major cause of infectious hepatitis worldwide [33]. The virus is characterized by its resistance to heat, acid pH, polar solvents, and

common disinfectants [57]. It is primarily transmitted by the fecal-oral route and is a principal agent of localized food-borne outbreaks of infectious hepatitis in developed countries [17]. The virus contains a single (+) stranded RNA genome that is approximately 7.4 kb long and contains a 3' poly (A) tail. The 5' end is uncapped but covalently linked to the viral coded protein VPg [65]. The viral genome has been cloned and sequenced from a number of strains. It codes for a single polyprotein, which is subsequently cleaved by the viral protease 3C and possibly cellular proteases into mature viral proteins [43, 54, 56].

Strains of HAV can be grouped into three categories based on their distinctive growth characteristics in permissive cells: i) wild-type (wt) strains, defined by a long incubation period between infection and detection of replication and a cytopathic effect (cpe) is not observed; ii) tissue culture adapted (cc) strains, defined by shorter incubation periods than for wt strains and cpe is not observed; and iii) tissue culture adapted (cp) strains, defined by shorter incubation periods than for cc strains and cpe is observed. The cp strains arise during repeated passage of cc strains in permissive cells [2, 7, 21, 25, 47, 62, 68]. Although the molecular basis for the development of the cp phenotype is poorly understood, it is well documented that both viral genome replication and viral protein expression can be detected much earlier in permissive cells infected with cp strains such as HM175/18f, HM175/24a and HM175/HB1.1, than in cells infected with the parental cc strains from which they were derived [7, 26, 29, 32, 42]. The rapid replication and viral gene expression observed for cp strains has been attributed to a more efficient initiation of translation from the IRES (internal ribosomal entry site) of cp strains due to mutations in this region [9, 28, 66], though some have disputed this interpretation [32, 38].

Apoptosis is observed following infection by a number of picornaviruses, especially when virus replication is restricted [1, 10, 60, 61]. While cell killing by apoptosis may aid in spreading progeny virus or escape cellular defense mechanisms [51], premature induction of apoptosis may limit virus growth and spread [4, 10, 51]. The cytopathic effect that is observed in cells following infection with cp strains of HAV has been attributed to the induction of apoptosis [7, 29]. Apart from the demonstration of a link between rapid replication and cytopathogenicity of the cp strains of HAV, the actual molecular events leading to apoptosis following infection with cp strains are unknown. Expression of P2 region proteins 2B and 2C from either cp or cc strains in FrhK4 cells result in the accumulation of a tubular-vesicular network [29, 37]. Expression of the P3 region protein 3AB has been shown to result in membrane alterations in bacterial cells with resultant changes in membrane permeability [50]. The lack of correlation between apoptosis and expression of either P2 or P3 region proteins prompted us to investigate alternative mechanisms of apoptosis induction by cp strains of HAV.

In this study, we report that infection of FrhK4 cells with the HAV cp strain HM175/18f results in the degradation of ribosomal RNA (rRNA) and the reduction of several cellular mRNAs including β -actin and GAPDH. Ribosomal RNA degradation was specific for the 18f strain and the fast replicating enterovirus coxsackievirus B1 (CBV1), while the parental cc strain of 18f did not induce rRNA

cleavage. The effect of 18f or CBV1 infection on rRNA integrity was observed in the absence of interferon (IFN) induction. Ribosomal RNA degradation was detected early after virus infection and prior to induction of cpe. This degradation was blocked by inhibitors of virus replication. The pattern of rRNA degradation suggests the involvement of the dsRNA activated RNase L; the regulation of this enzyme could provide an alternative mechanism by which 18f infection induces apoptosis.

Materials and methods

Cells and viruses

FrhK4 monkey kidney cell line was a kind gift of Dr. G. Kaplan (FDA, Center for Biologics Evaluation and Research, Bethesda, MD). The cells were grown in Eagles Minimal Essential Medium (EMEM, Life Technologies, Gaithersburg, MD) containing 5 % heat inactivated fetal bovine serum (FBS), MEM non-essential amino acids and sodium pyruvate (all from Life Technologies), with routine weekly sub-culturing. Under these conditions the cells increase in number about 20-fold in 6 to 7 days. The cell line is contact inhibited and can be kept in growth medium or maintenance medium (1 % FBS) for several weeks without degeneration of the monolayer. HAV strains HM175/18f and HM175/clone 1 [42, 68], and Human coxsackievirus B1 (CBV1) were obtained from ATCC. All three viruses were grown in FrhK4 cells. Virus stocks were prepared essentially as described [7, 29]. 18f and CBV1 were titered by plaque assay, while clone 1 virus was titered by an enzyme immunoassay (EIA) in 96 well plates as described previously [31] using the HAVAB EIA Diagnostic Kit (Abbott Laboratories, Abbott Park, IL).

Virus infection for RNA isolation

Confluent cultures of FrhK4 cells in 75 cm² flasks (5×10^6 cells) were infected with 5–10 pfu/cell of 18f or CBV, or 15 TCID₅₀ of clone 1 in 1.5 ml of MEM containing 1 % heat inactivated FBS or mock infected. After 1 h of adsorption, 13.5 ml of the same medium was added to each flask and incubation continued until the indicated times of cell harvest. Cells were harvested by scraping, centrifuged to remove medium, and the pellets washed once with PBS (Ca⁺⁺ and Mg⁺⁺ free) and either stored frozen at –70 °C or used immediately. For RNA isolation, cell pellets were dissolved in TRIZOL (Life Technologies) containing 100 mM β-mercaptoethanol (Sigma), following the protocol suggested by the manufacturer. All RNAs were routinely digested with RNase-free DNase (Promega, Madison, WI) in the presence of ribonuclease inhibitor (RNasin, Promega) for 30 min at 37 °C, followed by phenol/chloroform extraction and alcohol precipitation. RNAs were quantitated by UV absorption at 260 nm.

Treatment of cells with inhibitors of virus replication

Infected or mock infected cells were treated with 50 μg/ml cycloheximide, 2.5 mM Guanidine hydrochloride, or 5 μg/ml Brefeldin A in MEM containing 1 % FBS immediately following the virus absorption period. For measurement of virus replication, 12 well plates containing approximately 2.5×10^5 cells were used. Cells were fixed in methanol/PBS at 24 hpi and viral antigens detected by EIA [31]. For RNA isolation, 75 cm² flasks, containing approximately 5×10^6 cells at the time of infection were harvested at 24 or 48 hpi, and RNAs isolated as described above.

Persistent infection with HM175/clone 1

A 25 cm² flask was seeded with FrhK4 cells and infected at approximately 80 % confluence with clone 1 virus as described above. The virus was allowed to replicate for 7 days and thereafter the cells were trypsinized and seeded into a 75 cm² flask. Subsequently, the flask was sub-cultured at weekly intervals by trypsinization and seeding a new flask with one tenth of the cell suspension. To monitor virus replication, periodically cells were seeded into 12 well plates and cultured for 24 to 48 h until the plates were confluent. Cells were fixed in 80 % methanol and viral antigens were measured by the HAVAB EIA procedure [31]. Uninfected cells were used as a negative control.

Gel electrophoresis and Northern transfers

Samples of RNA (8 µg unless otherwise indicated) were denatured by heating at 55 °C for 15 min in 20 µl of buffer containing 1× MOPS buffer, 50 % formamide and 6.7 % formaldehyde. Samples were separated in a 1 % agarose gel containing 1× MOPS buffer, 0.41 M formaldehyde, and 1 µg/ml EtBr [16]. The gel was photographed under UV light and transferred overnight to Nytran N membranes (Schleicher & Schuell) in 20× SSC. The membrane was washed briefly in 2× SSC, baked under vacuum and stored at 4 °C prior to hybridization.

Hybridizations

Probes for β-actin and GAPDH were labeled by random priming of DECAtemplateTM-β-actin-mouse and DECAtemplateTM-GAPDH-mouse respectively (AMBION, Austin, TX), using α-³²P dATP (3000 Ci/mmol, ICN, Costa Mesa, CA). Probe for 18S rRNA was DECAtemplateTM-18S-mouse, also obtained from AMBION and was similarly labeled. The anti-sense RNA probe for the 28S rRNA (pTRI RNA 28S, Ambion) was labeled using SP6 polymerase and α-³²P UTP. The probe for HAV genomic RNA was obtained by *Xba* I digestion of the plasmid pHAV/7 (kindly provided by Dr. S. Emerson NIH, Bethesda, MD). Following gel purification, the large *Xba* I fragment, representing almost all of the genomic RNA (except the IRES), was labeled by nick translation using α-³²P dATP. Blots were prehybridized at 65 °C in Hyb-9 (Gentra) supplemented with denatured salmon sperm DNA or yeast tRNA (for the RNA probe) for 3–4 h with continuous agitation and hybridized with probe (2–3 × 10⁶ cpm/ml) overnight. Filters were washed once in 2× SSC/1 % SDS for 30 min and then 3 times in 0.1× SSC/0.1 % SDS for 30 min each time at 65 °C, prior to exposure to film or phosphorimager screen (Molecular Dynamics).

Preparation of antibody to HAV capsid protein VP1

Anti-VP1 antiserum was obtained from rabbits immunized with a synthetic peptide CVPETF PELKPGESRHT, corresponding to amino acids 64–79 of HAV viral capsid protein VP1, covalently linked to KLH. Synthetic peptide, free and KLH-conjugated, was purchased from New England Peptide, Inc (Fitchburg, MA). Pre-immune serum was collected from New Zealand white rabbits 1–2 days prior to immunization and stored at –70 °C. Rabbits were immunized with KLH-conjugated peptide emulsified in Freund's complete adjuvant and challenged at regular intervals, over a 14 to 19 week period, with KLH-conjugated peptide emulsified in incomplete Freund's adjuvant. The animals were hyperimmunized using unconjugated peptide resuspended in sterile PBS. The serum was collected and stored at –70 °C. All animal studies were conducted in compliance with the Guide for the Care and Use of Laboratory Animals under an approved IACUC protocol.

Protein extraction

Culture media was removed from mock or virus infected cell cultures and the monolayer were scraped into Ca^{++} and Mg^{++} free phosphate-buffered saline (PBS). Cells were pelleted ($1500 \times g$, 4°C) and washed twice with cold PBS. To obtain a total cell lysate, the cell pellet (while on ice) was resuspended in cold RIPA buffer (50 mM Tris-Cl, pH 8.0, 150 mM NaCl, 1 % NP-40, 0.5 % sodium deoxycholate, 0.1 % SDS) containing 1 mM PMSF, and 1:100 dilution of protease inhibitor cocktail (Sigma St. Louis, MO) and phosphatase inhibitor cocktails I and II (Sigma). Additional PMSF was added (1 mM) to the lysate prior to its passage through a 20 gauge needle (8–10 times). Following 30 min of incubation on ice, the sample was centrifuged at $10,000 \times g$ for 10 min 4°C to pellet insoluble material. The extracts were stored as aliquots at -20°C . Protein concentrations of lysates were estimated using the BCA-200 Protein Assay (Pierce Chemical Co., Rockford, IL) according to the manufacturer's instructions.

PAGE and Western blot Analysis

Sixty five μg of each protein extract were adjusted to equivalent volumes in denaturing sample buffer and heated at 95°C for 5 min and subjected to electrophoresis in SDS-10 % polyacrylamide gels followed by electrophoretic transfer onto supported nitrocellulose membranes (Optitran, BA-S 83, Schleicher and Schuell Inc.) in transfer buffer (25 mM Tris base, 192 mM glycine) containing 20 % methanol. The membranes were blocked with TBS-T (Tris buffered saline/0.1 % Tween 20) containing 5 % nonfat dried milk (NFDM) for 90 min at room temperature and washed four times with TBS-T. Using a mini-blotter manifold, membranes were incubated either overnight at 4°C with anti-STAT1 and anti-P-STAT1 antibodies (Cell Signaling Technologies, Beverly, MA) diluted 1:1000 in TBS-T containing 5 % BSA or 1 h at room temperature with anti-actin antibody (Sigma) and anti-VP1 antibody diluted 1:1000 in TBS-T containing 5 % NFDM. After four washes in TBS-T, the blots were incubated with goat anti-rabbit IgG-HRP antibody conjugate (Cell Signaling) diluted 1:2,000 in TBS-T containing 5 % NFDM. Following four washes at room temperature in TBS-T, the SuperSignal West Pico Chemiluminescent Substrate kit (Pierce Chemical Co. Rockford, IL) was used according to manufacturer's instructions followed by exposure to X-OMAT-XAR (Kodak, Inc.) for the detection of bound antibody-HRP conjugates.

^{35}S -labeling and SDS-PAGE

Cells were grown in 25 cm^2 flasks and infected when confluent with 18f as above and labeled at 72 hpi for 2 h with $50\ \mu\text{Ci/ml}$ of a mixture of ^{35}S -methionine and ^{35}S cysteine (ICN) in methionine and cysteine-free medium supplemented with 5 % dialyzed FBS (ICN) following a 30 min pre-incubation in methionine and cysteine-free medium. CBV1 infected cells and clone 1 persistently infected cells were labeled similarly at 7 h or 60 days post-infection (pi), respectively. Cells were collected by scraping, washed once with PBS and the pellets lysed in $200\ \mu\text{l}$ RIPA buffer containing protease inhibitors cocktail (Sigma). TCA precipitable incorporation was measured using $5\ \mu\text{l}$ of clarified lysate and protein concentration was measured with $2\ \mu\text{l}$ lysate. Labeled proteins were separated in a 4–20 % Novex pre-cast gel (Invitrogen, Carlsbad, CA), after heating the samples at 95°C for 3 min in $1 \times$ sample buffer containing dithiothreitol. Following electrophoresis, the gel was fixed and stained with Brilliant Blue G (Sigma) in 25 % methanol, 5 % acetic acid and destained in 25 % methanol, 5 % acetic acid. The gel was then treated with Amplify (Amersham Biosciences, Piscataway, NJ) for 30 min, dried and exposed to a phosphorimager screen, which was scanned in a Typhoon scanner (Molecular Dynamics).

Gene expression analysis

Total RNA preparations from mock infected, 18f infected (48 hpi), CBV1 infected (6 hpi), and HM175 infected (60 dpi) FrhK4 cells were labeled with α -³²P dATP using the CDS primers for human 1.2 array (Clontech, Palo Alto, CA), Clontech enzyme and reagents provided with the array. The labeled cDNA preparations were purified using the Nucleospin extraction kit (Clontech). Four identical arrays were pre-hybridized at 68 °C in hybridization bottles in a HYBAID oven (National Labnet, Woodbridge, NJ) in 10 ml of ExpressHyb (Clontech) containing 100 μ g/ml denatured sheared salmon sperm DNA (Eppendorf Scientific, Westbury, NY). Hybridization was performed overnight at 68 °C by the addition of denatured probe (1.5×10^6 cpm/ml) and 10 μ g human Cot-1 DNA (Clontech) directly to the pre-hybridization solution. The membranes were washed twice (30 min each) with $2 \times$ SSC-1 % SDS and twice (30 min each) with $0.1 \times$ SSC-0.5 % SDS at 68 °C, followed by a final wash at room temperature with $2 \times$ SSC for 5 min. The membranes were wrapped in Saran wrap and exposed to phosphorimager screens at room temperature for 24 to 48 h. The screens were scanned in a Molecular Dynamics Typhoon scanner at 100-micron resolution and analyzed using the AtlasImage 1.5 software (Clontech).

RT-PCR of viral RNA

1 μ gRNA samples were reverse transcribed in 20 μ l reactions using oligo (dT)₁₅ as the primer and AMV reverse transcriptase and 5 μ l of each cDNA pool were PCR amplified using primers BG 7 and BG 8 as described [31]. Ten μ l samples were withdrawn after 27 and 30 cycles and analyzed by agarose gel electrophoresis. Bands were quantitated by the ImageQuant program from Molecular Dynamics following scanning of the EtBr stained gel by a Typhoon phosphorimager.

Results*Effects of virus infections on cell morphology*

At a moi of 5–10 pfu/cell, the rapidly replicating cp strain HM175/18f of HAV (18f) induced cell rounding in FrhK4 cells within 48 h post-infection (pi) in approximately 10 to 15 % cells. The percentage of cells exhibiting cpe increased for the next 48 h, so that by 96 h, 70 to 80 % of the cells were rounded and detached from the surface of the culture flask. Thus, even with the 18f virus, infection is characterized by a slow and asynchronous recruitment of cells into supporting viral replication. Similar effects have been reported for other cp strains of HAV, namely HM175/24a, and HB1.1 [7, 29]. In agreement with these results, we confirmed the induction of apoptosis in 18f infected FrhK4 cells by a colorimetric TUNEL assay (data not shown). The parental HM175/clone 1 virus (clone 1), also used in the present study, produced no changes in cell morphology after several months of continuous culture of infected cells, although viral antigens could be detected by EIA after four weeks of weekly subculture following the initial infection. The coxsackie virus strain B1 (CBV1) used in this study replicated very rapidly in FrhK4 cells, producing marked cpe within 7 hpi and all cells were floating by 14 to 15 hpi.

Cleavage of 18S rRNA after virus infection

We observed the appearance of RNA bands in the region between the 28S and 18S species, as well as below the 18S rRNA band, upon denaturing agarose gel electrophoresis of total RNA preparations isolated from 18f-infected cells (Fig. 1). The apparent degradation products were easily detectable after ethidium bromide (EtBr) staining of formaldehyde-agarose gels (Fig. 1A). RNA degradation was observed only in 18f infected cells at 48 and 96 hpi (lanes 3 and 4), while no degradation was observed at 96 hpi in clone 1 infected cells (lane 2) or mock-infected cells (lane 1). Degradation of rRNA has not been reported previously in HAV infected cells, therefore, the rRNA origin of the observed degradation

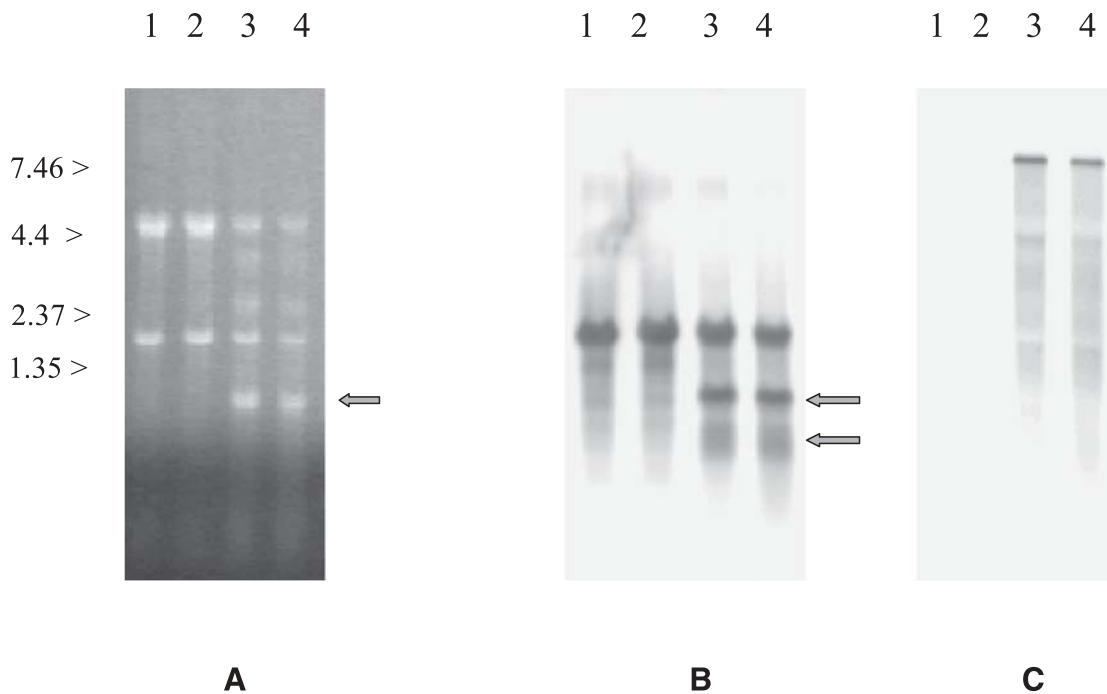


Fig. 1. Degradation of 18S rRNA in HM175/18f infected FrhK4 cells. Total cellular RNAs were extracted by the TRIZOL procedure, quantitated by A260 measurement, and 8 μ g of each RNA was separated in formaldehyde-agarose denaturing gels containing 1 μ g/ml ethidium bromide. The gel was transferred to Nytran membranes for hybridization. **A** Ethidium bromide stained gel. **B** Northern blot of panel A hybridized with an 18S RNA probe. **C** Northern blot of A hybridized with a probe for HAV RNA. 1, mock infected (96 h) cells; 2, HM175/clone 1 (15 TCID₅₀/cell) infected cells (96 hpi); 3 and 4, HM175/18f (10 pfu/cell) infected cells at 48 h and 96 hpi respectively. The probe for 18S RNA was a 1.2 kb fragment of the mouse 18S RNA gene (nucleotides 505 to 1694), labeled by random priming with α -³²P dATP. The probe for HAV genomic RNA was the large *Xba* I fragment from a genomic clone pHAV/7, labeled by nick translation with α -³²P dATP. An RNA ladder (0.24 to 9.5 kb) was included in the analysis and the position of the 1.35 to 7.4 kb fragments identified in panel A. An arrow is used to identify the putative 18S rRNA degradation product in **A** and the position of the 18S RNA and its degradation products in **B**. Full length HAV RNA is 7.5 kb (**C**)

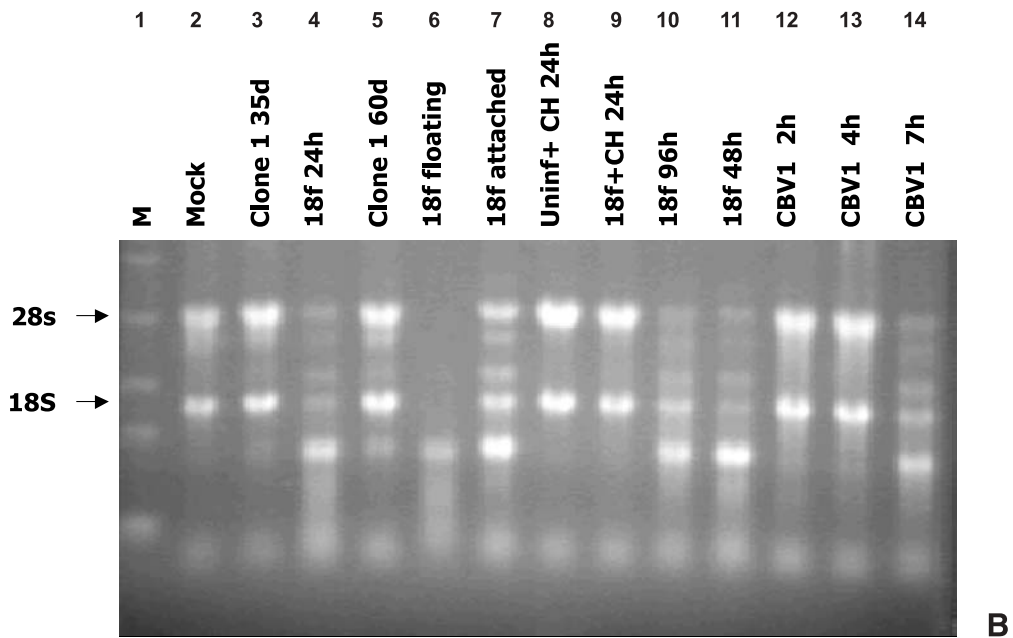
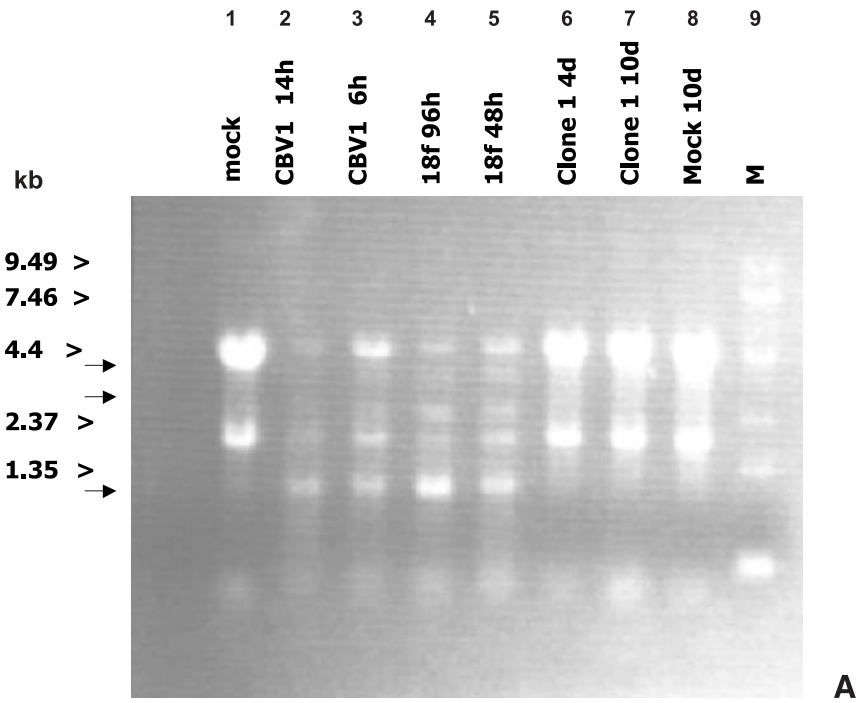
products was confirmed by Northern blot analysis. Duplicate RNA samples were electrophoresed and transferred to Nytran N membranes. One half of the blot was hybridized to a probe for 18S RNA (Fig. 1B), and the other half to a probe for HAV RNA (Fig. 1C). The 18S probe hybridized to intact 18S RNA and to two additional species of RNA (indicated by arrows) from 18f infected cells, while these species were not detected in RNA preparations from either mock or clone 1 infected cells. Apparently full length HAV RNA (7.4 kb) was detected in 18f infected cells at both 48 and 96 hpi, while no viral RNA was detected in clone 1 infected cells at 96 hpi, confirming that the 18f virus indeed was a faster replicating strain.

Cleavage of 28S rRNA in 18f and CBV infected cells

To further investigate whether RNA degradation was specific for 18f infection, and to determine the temporal relationship between RNA degradation and onset of cpe, we isolated total RNA from cells infected with CBV1, HM175/clone 1, and HM175/18f at different times, and analyzed them by formaldehyde-agarose gel electrophoresis (Fig. 2). In CBV1 infected cells, degradation of both species of rRNA was observed after CBV1 infection at 6–7 hpi, when almost all the cells in the monolayer were rounded but still attached to the surface (Fig. 2A, lane 3; Fig. 2B, lane 14). No RNA degradation was observed in CBV1 infected cells after 2 or 4 hours of infection (Fig. 2B, lanes 12 and 13 respectively). At 14 hpi, when all the cells have detached from the surface of the flask, very little intact 28S or 18S RNAs were observed (Fig. 2A, lane 2). Thus, in CBV1 infected cells, RNA degradation coincides with the appearance of cpe. In 18f infected cells, the extent of rRNA degradation increased during the period of 48 to 96 hpi, while rRNA degradation was not observed in clone 1 infected cells even at 10 dpi (Fig. 2A, lanes 4 and 5 vs. lane 7). RNA degradation was apparent in 18f-infected cells as early as 24 hpi (Fig. 2B, lane 4), although no gross effect on cellular morphology was visible at this time. In FrhK4 cells persistently infected with the cc strain HM175 (clone 1), RNA analysis after 35 days from the initial infection showed

Fig. 2. Degradation of rRNAs in FrhK4 cells infected with the 18f strain of HAV or the B1 strain of coxsackievirus (CBV1). **A** Confluent monolayers were infected with 10 pfu/cell CBV1 (2 and 3), 10 pfu/cell HM175 strain 18f (4 and 5), or 15 TCID₅₀/cell HM175/clone 1 (6 and 7). Total RNA was isolated at 14 hpi (2) or 6 hpi (3) from CBV1 infected cells; at 96 h (4) or 48 hpi (5) from 18f infected cells; at 4 d (6) or 10 dpi (7) from clone 1 infected cells. 1 and 8 show RNA from mock-infected cells at 48 h and 10 d, respectively. 9 is a 0.24 to 9.5 kb RNA ladder (*M*). Samples were separated in a denaturing agarose gel containing ethidium bromide. In 2, 2 µg of RNA was applied, while all the other lanes were loaded with 8 µg of RNA. **B** 1, 0.24 to 9.5 kb RNA ladder; 2, RNA from mock infected (24 h) cells; 3 and 5, RNA from persistently clone 1 infected cells at 35 and 60 days pi respectively; 4, 10 and 11, RNA from 18f infected cells at 24, 96 and 48 hpi, respectively; 6 and 7, RNA from floating and attached cells after 18f infection for 48 h; 8 and 9, RNA from mock or 18f infected cells following treatment with 50 µg/ml cycloheximide (CH) for 24 hpi; 12, 13, and 14, RNA from CBV1 infected cells at 2, 4, and 7 hpi respectively

little evidence of RNA degradation (Fig. 2B, lane 3), though small amounts of degradation products may be detected at 60 days following infection (Fig. 2B, lane 5). The levels of viral RNA and protein in clone 1 infected cells at 35 and 60 days pi were comparable to those observed in 18f infected cells, as measured by



RT-PCR and Western immunoblotting (Fig. 5) and EIA (data not shown). We have continuously cultured the persistently clone 1 infected cells for over five months without significant changes in cell morphology or rRNA integrity. When RNA was obtained from 18f-infected monolayers following separation of the rounded cells from cells with a normal morphology by vigorous agitation, rRNA degradation was apparent in both populations of cells (Fig. 2B, lanes 6 and 7). In lane 6, only 3 μ g of RNA was applied, since the percentage of floating cells at 48 hpi was low and the yield of RNA much less compared to the cells that remained attached (Fig. 2B, lane 7). In lane 6, no intact 28S or 18S bands were visible, indicating that almost complete degradation of the rRNA species has occurred in these cells. It should be noted that CBV1 infection proceeds much faster and synchronously in FrhK4 cells. Since we did not examine rRNAs from CBV1 infected cells between 4 and 6 hpi, it is quite possible that RNA degradation occurs in CBV infection prior to the onset of morphological changes associated with cpe.

To confirm that 28S rRNA degradation was occurring after infection with 18f or CBV1, a Northern blot of the RNA gel shown in Fig. 2 (panel A) was hybridized to a probe specific for 28S rRNA (Fig. 3). The short probe (115 bases from the 3' end of the 28S RNA) hybridized strongly to a fragment migrating faster than the 1.35 kb marker, as well as to intact 28S rRNA, but did not hybridize to apparent

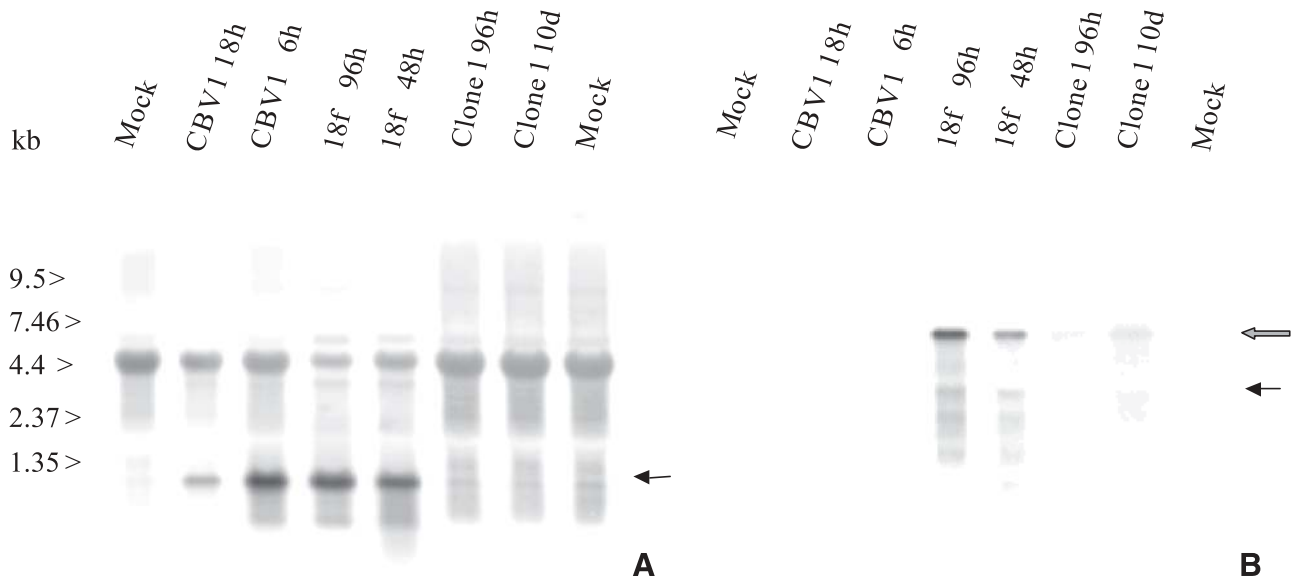


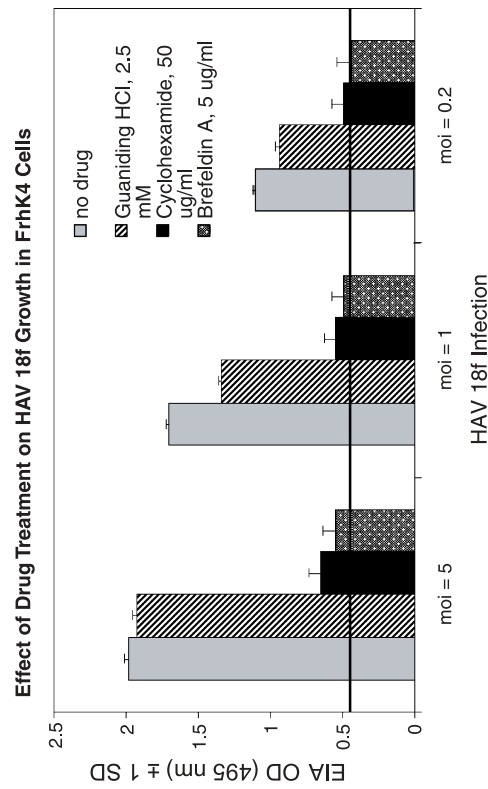
Fig. 3. Degradation of 28S rRNA and viral RNA in virus infected cells. **A** The RNA samples described in Fig. 2A were subjected to denaturing agarose gel electrophoresis. The gel was Northern blotted and hybridized to a labeled anti-sense RNA probe specific for 28S rRNA (nucleotides 4515 to 4400). The probe was synthesized from pTRIRNA-28S by transcription with the SP6 polymerase. The arrow indicates the position of a 28S RNA degradation product. **B** An identical Northern blot was hybridized to a nick translated DNA probe for HAV as described in Fig. 1. Arrows indicate position of full-length HAV RNA (7.5 kb) and putative degradation products

degradation products seen in EtBr stained gels (Figs. 1 and 2) that migrated to the region between the 28S and 18S species. It is likely that these latter products were derived from the 5' end of the 28S rRNA and could not be detected by a probe targeted to the 3' end. Nevertheless, it is clear that both the large and small rRNA molecules were degraded in CBV1 and 18f infected cells, and that this degradation coincided with the appearance of cpe in CBV1 infected cells but preceded the appearance of cpe in 18f-infected cells. In contrast, infection of permissive cells with mouse hepatitis virus (a coronavirus) resulted in the degradation of only the 28S species [3]. Apparently intact HAV RNA was detected in 18f-infected cells at 48 hpi and 96 hpi, and, albeit at lower levels in clone 1 infected cells at 10 dpi (Fig. 3B). This blot was exposed longer to reveal the existence of HAV RNA in clone 1 infected cells. While overexposure of the blot showed that some degradation of viral RNA might also be taking place, the bulk of the viral RNA remains intact, possibly protected from degradation by its association with capsid proteins. On the other hand, the smaller virus specific RNA molecules could have resulted from premature termination of transcription [48].

Effects of inhibitors on virus replication and RNA degradation

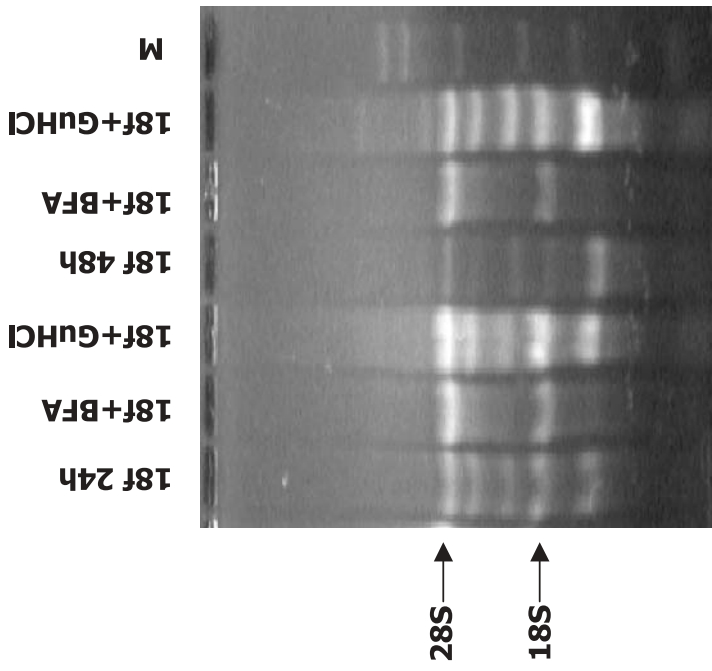
To investigate whether the degradation of rRNAs observed in 18f infected cells required replication of the virus, we studied the effects of several inhibitors of virus replication on RNA degradation. Cyclohexamide (CH) is a strong inhibitor of protein synthesis in many cultured cell lines and produces a marked cpe in treated cells that is attributed to induction of apoptosis [1, 7]. In agreement with the results of Brack et al. [7], we observed 18f-like cpe after treatment of FrhK4 cells with CH at concentrations ranging from 10 to 50 $\mu\text{g/ml}$. Despite the induction of cpe/apoptosis, CH treatment failed to elicit RNA degradation in uninfected FrhK4 cells (Fig. 2B, lane 8), and inhibited both virus replication (Fig. 4A), and degradation of RNA in 18f infected cells (Fig. 2B, lane 9). The inhibition of virus replication was not unexpected since CH inhibits picornavirus genome replication by preventing translation of input genome to produce viral RNA dependent RNA polymerase [1].

Brefeldin A (BFA) has been shown to induce apoptosis in other cell lines through the activation of caspase and disruption of Golgi complex function, and to inhibit replication of HAV and some picornaviruses, as well as viral RNA synthesis [5]. Treatment of FrhK4 cells with 5 $\mu\text{g/ml}$ BFA produced marked apoptosis within 24 h while suppressing 18f replication and 18f induced RNA degradation (Fig. 4, panels A and B respectively). Thus, RNA degradation in 18f-infected cells was prevented by both CH and BFA. CH and BFA induced apoptosis in FrhK4 cells was synchronous and was complete by 24 h as evidenced by cell rounding and eventual detachment from the growth surface. However, these changes were not accompanied by RNA degradation following treatment with either CH (Fig. 2B) or Brefeldin A (data not shown). Treatment of 18f-infected cells with 2.5 mM guanidine hydrochloride (GuHCl), on the other hand, had a marginal effect on 18f replication at high moi, and a somewhat larger effect at low moi (Fig. 4A). However,



A

Fig. 4. A Effect of drug treatment on HAV 18f growth. FrhK4 cells were grown to 95 % confluency in 12 well tissue culture plates and infected with HAV 18f at an moi of 0.2, 1 or 5 in MEM containing 1 % FBS or mock infected with MEM containing 1 % FBS. Following a 2 hour virus adsorption, MEM containing 1 % FBS alone or supplemented with either guanidine HCl, cyclohexamide or Brefeldin A was added to the cultures. At 24 h post-infection, the culture medium was removed and the monolayers washed twice with PBS. After fixation in cold methanol, the monolayers were analyzed for viral growth by EIA as described under Materials and methods. The results of duplicate and triplicate experiments were plotted as mean EIA OD_{495 nm} ± 1 standard deviation (SD) for virus infected cells treated or not with the drug indicated, and the value for mock infected, untreated cultures (0.408 ± 0.014) plotted as a solid horizontal line. Statistical significance between the means of untreated and drug treated, infected cultures was determined using the Student's t-test (one-tailed). Significance at *p* < 0.0005 exists for treatment with cyclohexamide or Brefeldin A, while a significance at *p* < 0.005 exists for guanidine HCl only at an moi of 1 and 0.2. **B** Effect of drug treatment on RNA degradation in HAV 18f infected cells. FrhK4 cells were cultured and infected with HAV 18f at a moi of 5 (or mock infected) as described in **A** and then treated (or not) for the duration of infection with either Brefeldin A (BFA) or Guanidine HCl (GuHCl). Cells were harvested at 24 and 48 hpi for isolation of RNA and analysis by agarose gel electrophoresis. An RNA ladder (M) was included in the gel. The positions of 28S and 18S rRNAs are indicated by arrows



B

GuHCl treatment did not prevent RNA degradation in 18f-infected cells (Fig. 4B). It has been reported that GuHCl, an inhibitor of poliovirus replication, is ineffective against HAV due to a mutation in the genome [18], but GuHCl was found to be a strong inhibitor of HM175/p39 virus [15]. These experiments clearly show that in FrhK4 cells, replication of the 18f virus is required for RNA degradation, and that degradation of RNA is not a consequence of apoptosis.

Viral RNA and protein in persistently clone 1 infected FrhK4 cells

Degradation of rRNA is a feature of virus infection in interferon (IFN) treated cells and is believed to be due to the availability of double stranded RNA (dsRNA) during replication or transcription of the viral genome, resulting in the activation of the RNase L pathway [58, 59]. However, in the absence of IFN pre-treatment, dsRNA can activate the RNase L pathway by activating pre-existing 2-5A synthetase, which ultimately results in cell death [35, 36, 52]. Since viral RNA replication and expression occurs much earlier post infection in 18f-infected cells compared to clone 1 infected cells, the degradation of rRNAs could result from an early dsRNA dependent activation of RNase L in 18f-infected cells. We further investigated whether the lack of RNA degradation and cpe in clone 1 infected cells observed at later times pi may correlate with diminished levels of viral RNA or protein. FrhK4 cells were infected with HM175/clone 1, and the cells were serially passaged at weekly intervals until viral antigens were detectable by EIA (data not shown). After 35 days, the level of viral antigens was comparable to that observed in 18f infected cells after an acute infection. Total cellular RNA, and proteins were isolated from the persistently infected cells. The level of viral RNA in the persistently infected cells was measured at 35 and 60 days of continuous culture by RT-PCR (Fig. 5A). The level of viral RNA was somewhat lower in clone 1 infected cells after 35 days, but at 60 days the levels were almost the same as in 18f infected cells at 48 hpi. PCR amplification was carried out for 27 and 30 cycles to ensure that the signal strengths of the PCR products were obtained before the reactions reached saturation (27 cycles). Western blot analysis with anti-VP1 antibody also showed lesser but easily detectable accumulation of the viral capsid protein VP1 in persistently clone 1-infected cells (Fig. 5B). However, the cells did not show any discernable morphological change after more than 120 days of weekly subculture and produced viral antigens and RNA as determined by EIA and RT-PCR. The data indicate that, unlike 18f infection, clone 1 replication and expression does not induce rRNA degradation.

β -actin and GAPDH levels in virus infected cells

A reduction in cellular RNA and protein levels during virus infection may aid in the replication of viruses possessing a cp phenotype (e.g., HAV HM175/18f), or a rapid growth/cpe characteristic (e.g., CBV) in cell lines permissive for virus growth. For example, translation of HAV RNA in infected cells requires interaction of trans-acting cellular protein factors with cis-acting elements present at the 5'

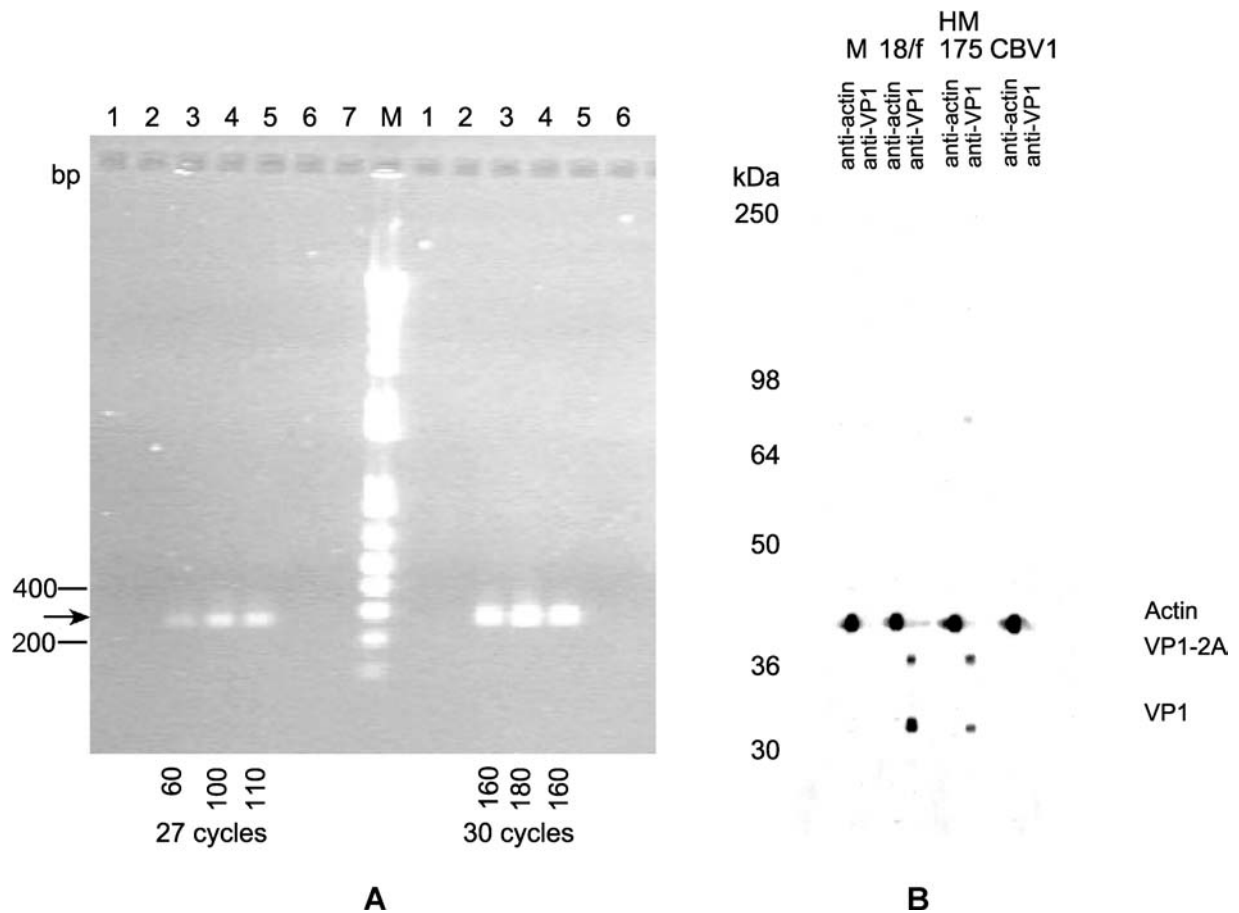


Fig. 5. A RT-PCR detection of HAV genomic RNA in acute and persistently infected FrhK4 cells. 1 μ g of each total RNA sample was reverse transcribed in 20 μ l, and 5 μ l of the resulting cDNA pool was PCR amplified with primers specific for HAV to amplify a 276 bp region from the 3' end of the genome (nucleotides 6850 through 7125). The position of the 276 bp amplicon is indicated by arrow. Samples (10 μ l) were withdrawn after 27 and 30 cycles, mixed with loading buffer and applied on a 1% agarose gel. 1, RT-PCR control reaction; 2, 48 h mock infected FrhK4 cells, 3 is clone 1-infected cells at 35 days pi, 4 is 18f infected cells at 48 hpi, 5 is clone 1 infected cells at 60 days pi. 6 and 7 are negative controls where total cellular RNA was replaced with transfer RNA from *E. coli*. M is a 1 kb plus ladder (Life Technologies). 1–6 to the left of the marker (M) lane are results after 27 cycles of amplification, and 1–6 to the right are the results after 30 cycles of amplification. The gel was photographed using a FOTODYNE system with a CCD camera. Pixel values were obtained for visible band area using the ImageQuant program (Molecular Dynamics). **B** Western blot analysis of virus infected cell extracts for the detection of VP1 and actin. Protein extracts were prepared from coxsackie B virus infected cells at 7 hpi (CBV1), from 18f infected cells at 72 hpi (18f), from clone 1 infected cells at 35 dpi (HM175), and from 72 h mock infected cells (M) cell pellets as described in Materials and methods. Sixty-five μ g of each protein extract was subjected to electrophoresis on SDS-10% polyacrylamide gels followed by electrophoretic transfer onto supported nitrocellulose membranes. Detection of VP1 and actin with specific antibodies were performed as described under Materials and methods. The positions of VP1 and actin are identified with arrows. VP1-2A is a precursor of mature VP1

Interferon is not involved in the RNA degradation process

The degradation of rRNA into discrete products is a hallmark of the antiviral effect of interferon. Since the cell line used for these experiments was not treated with interferon prior to virus infection, it was important to determine whether the FrhK4 cell line is a natural producer of interferon, or if interferon is induced as a result of virus infection. To investigate if interferon mRNAs were present in FrhK4 cells prior to or following virus infection, nylon arrays, each containing 1176 human genes including those for interferons α , β , and γ were hybridized to cDNA probes synthesized using total RNA from uninfected and virus infected cells as templates. Surprisingly, we did not find significant hybridization signals

Table 1. Induced and down-regulated genes during 18f infection of FrhK4 cells. Array hybridizations were carried out in duplicate with cDNA probes prepared using two independent RNA preparations each from mock and virus infected FrhK4 cells. Independent phosphorimager scans for each duplicate sample (control or infected) were averaged using AtlasImage program to produce composite arrays for control and infected cells. The composite arrays were then compared to detect differences in signal levels using AtlasImage software. Gene signal values that were less than two-fold over background values were considered insignificant. Ratios of less than one represent down-regulation in the infected cells. Ratios of higher than one represent up-regulation in the infected cells. A less than two-fold difference of signal intensity between control and infected samples are considered insignificant. ND means the pixel value for that gene was equivalent to background

Gene description	Clone 1	18f	CBV
1. c-Jun; transcription factor AP-1	0.20	3.59	0.58
2. c-myc oncogene	0.98	1.80	2.65
3. Nerve growth factor; neurotrophic factor	0.70	0.48	1.00
4. EGF response factor 1	0.78	1.80	0.64
5. DNA binding protein inhibitor Id-2	1.42	3.11	0.53
6. Early growth response protein (Egr-1)	0.32	0.40	0.38
7. Nuclease sensitive element DNA binding protein	1.94	0.57	0.93
8. IL-2 receptor alpha subunit precursor	1.80	2.70	3.00
9. Glutathione S-transferase pi	1.50	0.75	0.61
10. Adenosine A 1 receptor	1.16	1.10	1.00
11. Apoptosis regulator bcl-x	2.23	1.10	1.00
12. ICE-like apoptotic protease 4 (caspase 10)	0.64	0.75	1.00
13. Macrophage specific colony stimulating factor	0.47	1.80	0.77
14. Vascular endothelial growth factor precursor	0.48	0.68	0.62
15. Thymosin β -10	1.10	0.64	1.02
16. Alpha-1 antitrypsin precursor	0.10	0.14	0.03
17. Thymosin β -4	1.50	0.74	0.99
18. Cathepsin D precursor	0.33	0.30	0.24
19. Interferon- β	ND	ND	ND
20. Interferon- α 2	ND	ND	ND
21. Interferon- γ	ND	ND	ND

Note: Changes in levels are relative to Uninfected FrhK4 cells. ND = Not detected

corresponding to the interferon genes in either uninfected or HAV infected cells (Table 1). These results are supported by the data from Pietiäinen et al. [49] suggesting that IFN mRNAs are neither present nor induced during PV1, EV1 and CBV4 infection of HOS and HeLa cells. However, low levels of IFN RNAs, and any comparative differences between uninfected and infected cells, may not be detectable by array hybridization. RT-PCR analysis of total RNA from virus

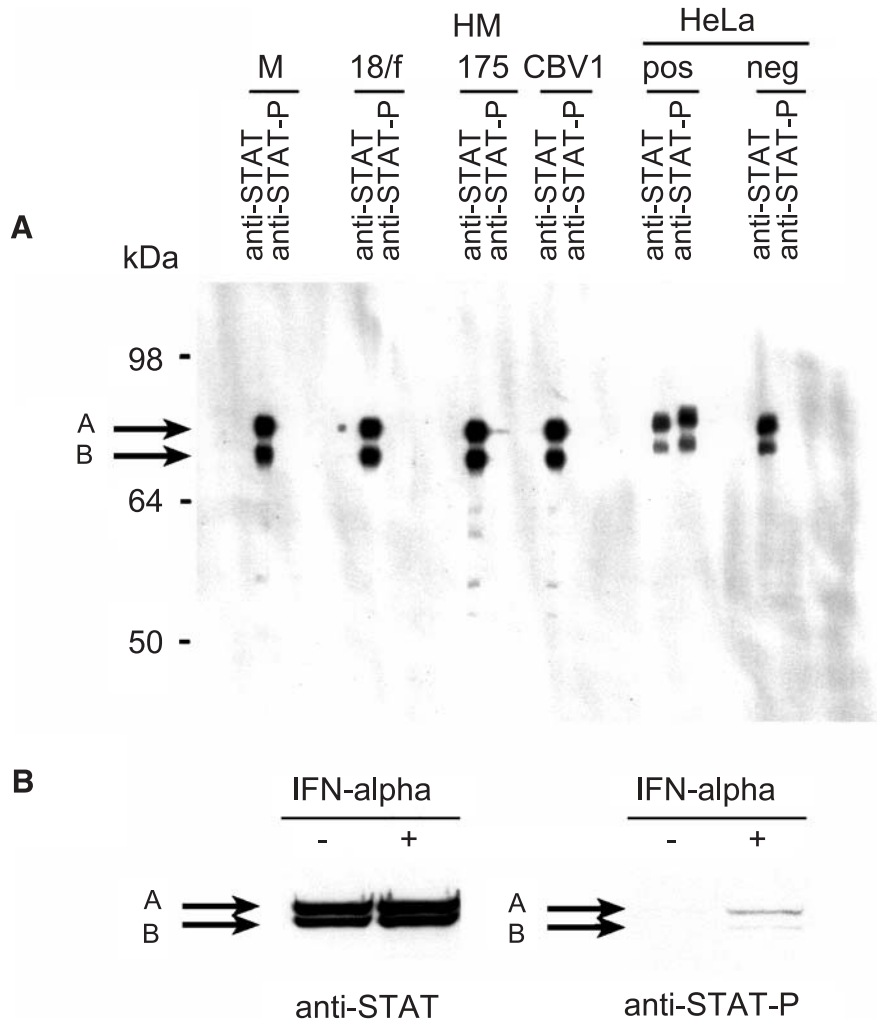


Fig. 7. Western blot analysis of virus infected cell extracts for the detection of STAT1 and phosphorylated STAT1. Protein extracts were prepared, subjected to SDS-10% PAGE and electrophoretic transfer, and analyzed by Western blotting as described in Fig. 5B, except incubation with primary antibody was overnight at 4 °C with anti-STAT1 and anti-STAT1-P antibodies diluted 1:1000 in TBST containing 5% BSA. Proteins extracts from untreated (neg) and IFN treated (pos) HeLa cells (Cell Signaling Technology, Inc., A) and from untreated (-) and IFN treated (+) FrhK4 cells (B) were used as negative and positive controls for STAT1 phosphorylation, respectively. The two splice variants of STAT1 (A and B) are indicated by arrows. HeLa STAT1 proteins migrate as slightly larger molecules. Phosphorylation results in an upward shift of both splice variants in the positive control

infected FrhK4 cells did not show increased level of β -IFN mRNA compared to uninfected cells. However, treatment of these cells with dsRNA resulted in β -IFN mRNA induction (data not shown). We investigated the possibility that low levels of IFN may be present in control or infected FrhK4 cells by looking at the phosphorylation status of STAT1 by Western immunoblotting (Fig. 7). Signal transducer and activator of transcription (STAT) 1 and 2 are regulators of IFN-induced gene expression. In cells treated with IFN, both STAT1 and STAT2 are phosphorylated by Janus kinase (JAK), which is a prerequisite for dimerization and translocation to the nucleus [58, 59]. The antibody to STAT1 readily detected the two forms of this protein in both control and virus infected cells, as well

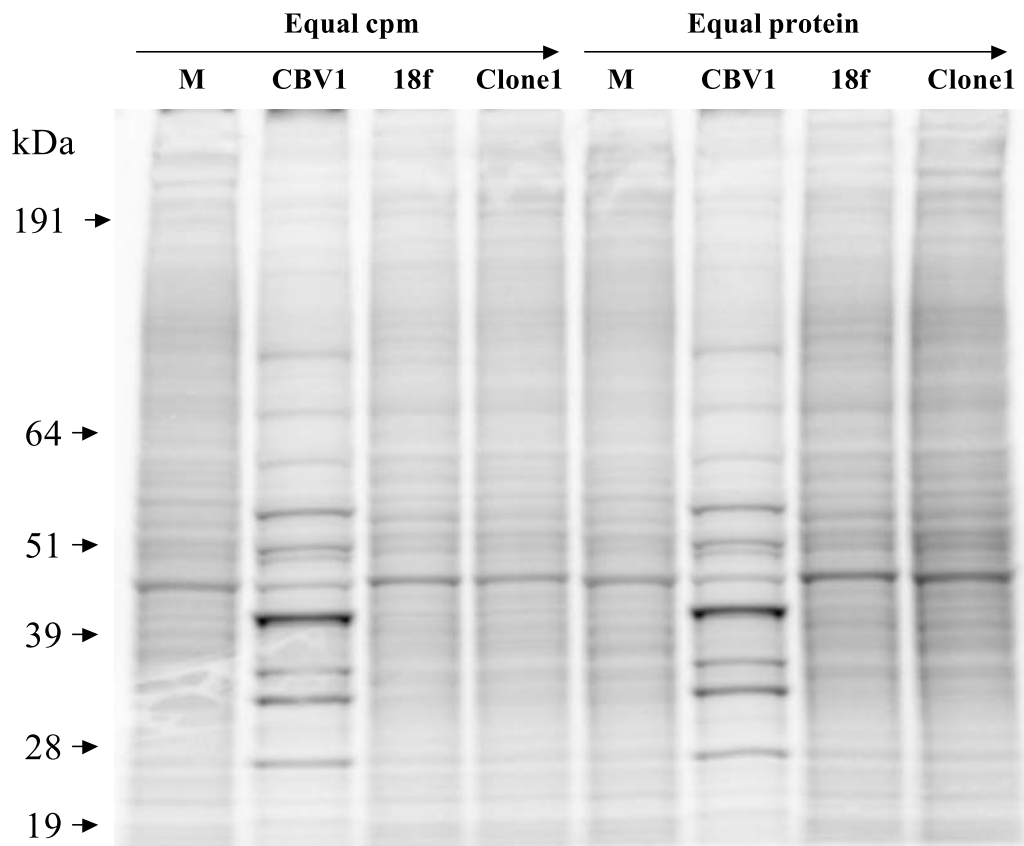


Fig. 8. Protein synthesis in control and infected FrhK4 cells. Cells were labeled for 2 h in methionine and cysteine free medium supplemented with $50 \mu\text{Ci/ml}$ of a mixture of ^{35}S methionine and ^{35}S Cysteine, and 1 % dialyzed FBS. Labeling was carried out in 25 cm^2 flasks at 7 hpi for CBV1 infected cells, 72 hpi for 18f infected cells, at 60 days pi for clone 1 infected cells, as well as after mock (*M*) infection (72 h). Volumes of extracts containing equal number of cpm or protein were heated in SDS sample buffer containing reducing agent prior to loading on a 4–20 % polyacrylamide gel that was run in MOPS-SDS buffer along with molecular weight markers. The gel was stained, destained and, and treated with Amplify (Amersham) prior to drying according to standard protocol and exposed to phosphorimager screen, which was scanned by a Typhoon scanner

as in control and interferon treated HeLa cell extracts. Both STAT1 proteins in HeLa migrate as slightly larger molecules. Using an antibody specific for the phosphorylated STAT1, STAT1 phosphorylation was not detected in either control or 18f-infected FrhK4 cells (Fig. 7), confirming the results obtained by array hybridization. In addition, STAT1 phosphorylation was not observed in CBV1 infected FrhK4 cells while phosphorylated STAT1 was readily detected in IFN treated HeLa cells (Fig. 7, panel A), and FrhK4 cells (Fig. 7, panel B). These results are in agreement with those obtained by array hybridization, indicating that IFN is not expressed and, therefore, is not mediating RNA degradation in 18f-infected cells.

Protein synthesis in virus infected cells

Unlike most enteroviruses, even cp strains of HAV lack the ability to shut off host protein synthesis. This inability to cause host shut-off is most likely due to a non-functional 2A protease, and is probably a major reason for the slow growth phenotype of HAV [34]. While it would contradict published reports, it seemed possible that 18f induced RNA degradation could result in host shut-off triggered by events peculiar to FrhK4 cells. Therefore, we investigated the effect of 18f infection on overall protein synthesis by pulse labeling of cells for 2 h and analysis of the products by SDS-polyacrylamide gel electrophoresis (SDS-PAGE). As shown in Fig. 8, CBV1 infection resulted in a dramatic reduction of cellular protein synthesis at 7 hpi, and viral proteins could be clearly identified. In contrast, the effect of 18f infection was much less pronounced, and comparable to the effect of the parental cc (clone 1) strain. Thus no positive identification of HAV specific proteins could be made from such an analysis. It should be noted that the clone 1 infected cells used for protein labeling in this experiment have been routinely sub-cultured for more than two months, and were actively producing viral antigens as detected by a colorimetric EIA procedure (data not shown) as well as viral RNA and VP1 capsid protein (Fig. 5). However, RNA degradation was not evident in these cells. In conclusion, rRNA degradation alone is not sufficient for host shut-off.

Discussion

Cytopathic (cp) strains of HAV have been isolated in several laboratories during the past few years. The cp strains arise during repeated passage of cc strains in permissive cells and the genetic basis for the development of the cp phenotype is poorly understood [2, 7, 21, 25, 47, 62, 68]. There is no evidence to indicate conclusively which nucleotide changes arising in the cp genotype are responsible for both the rapid growth and the cp phenotype [23, 26, 29, 38, 42, 68]. These characteristics may be the result of different mutational events that have occurred during cc strain replication.

The data presented here identify a previously unreported event that occurs during infection with a cp strain of HAV, namely the degradation of rRNAs and the reduction in the level of cellular RNAs. Similar effects on rRNA, and β -actin

and GAPDH mRNAs were also observed after CBV1 infection. However, the non-cpe inducing parent strain of 18f, HM175/clone 1 had only a marginal effect on rRNA integrity during long-term persistent infection. Similar to the effects of enteroviruses, such as PV1, CBV4 and EV1, on the expression of certain cellular genes involved in apoptotic pathways, c-myc and c-jun levels were moderately increased in 18f-infected cells, while c-jun level was markedly reduced in clone 1 infected cells (Table 1). Full length viral RNA was detectable much earlier in 18f-infected cells compared to cells acutely infected with the clone 1 virus (Figs. 1 and 3). Significantly, viral RNA and viral capsid protein VP1 were present at comparable levels following extended culture of clone 1-infected cells in the absence of significant RNA degradation (Fig. 5).

Degradation of rRNA following infection of interferon treated cells has been reported for a number of DNA and RNA viruses [58, 59]. Moreover, dsRNA, a likely intermediate of RNA virus replication or transcription, has been shown to promote rRNA degradation without interferon treatment in some cell lines [6, 12, 35, 36, 45, 52, 53, 64, 69]. The function of dsRNA as an effector of the interferon response is dependent on both the cell type and the nature of the virus [58, 59]. For example, vaccinia virus is known to evade the effects of IFN treatment, but in suspension cultures of mouse L929 cells treated with IFN, rapid degradation of rRNA was observed [30]. Activation of the 2-5A/RNase L pathway has been reported during estrogen withdrawal from chick oviducts [19]. The enzyme responsible for the synthesis of 2-5A, 2'-5'-oligoadenylate synthetase can apparently be also induced by hepatitis C virus coat protein [46]. While the role of a viral protein in the activation of 2-5A/RNase L pathway in 18f or CBV1 infected FrhK4 cells cannot be ruled out, previous reports with EMC virus and the studies involving dsRNA clearly suggests a similar mechanism of rRNA degradation reported here. It remains unclear why rRNA degradation and apoptosis are absent in clone 1 infected cells despite the presence of viral RNA and protein. Perhaps cellular inhibitors of RNase L play a role in blocking RNA degradation in clone 1 infected cells [44]. It is also possible that a mechanism, analogous to the adenovirus VAI RNA mediated inhibition of PKR activity is used by the clone 1 virus to disarm the RNase L pathway [58, 59]. Clearly, accumulation of sufficient viral RNA or proteins cannot account for either rRNA degradation or the cp phenotype, since cc strains accumulate enough viral RNA and proteins after an initial lag (Fig. 5). It is interesting to note that while the precursor of mature VP1 protein VP1-2A is present in equal amounts in both 18f and clone 1 infected cells, VP1 itself accumulates to higher levels in 18f infected cells, suggesting a slower processing of the precursor in clone 1 infection. Surprisingly, we did not see a general inhibition of protein synthesis in FrhK4 cells infected with the cp (18f) strain of HAV despite massive RNA degradation, although an almost total shutoff of host protein synthesis was observed in CBV infected FrhK4 cells (Fig. 8). This is in contrast to the general inhibition of protein synthesis observed upon activation of the RNase L pathway in some cell lines [11, 12, 30, 35, 36, 52, 69]. The effect of CBV infection on protein synthesis is most likely a combination of rRNA cleavage (this study) and cleavage of eIF4G, poly (A)-binding

protein (PBP), and other translation factors mediated by an active 2A protease [10, 39, 41].

It has been shown that both caspase activation and apoptosis induction can occur when 2'-5'A synthetase is activated and rRNA degradation is induced [11, 12, 24, 52, 69]. While we have not directly assessed the level of 2-5A following virus infection, no other RNase currently known produces the characteristic degradation pattern of rRNA that we have observed. It is apparent from our data, however, that RNA degradation is dependent upon cp virus strain replication, since compounds, such as cycloheximide and Brefeldin A, that inhibited 18f replication also abolished rRNA degradation in 18f infected cells (Figs. 2 and 5). Treatment in the absence of infection did not induce RNA degradation. Additionally, the treatment of uninfected cells with these compounds induced apoptosis in the absence of RNA degradation (Figs. 2 and 4). In view of the temporal relationship between onset of rRNA degradation and induction of cpe/apoptosis, these results suggest that RNA degradation following 18f (or CBV1) infection is the cause, rather than the effect, of apoptosis. On the other hand, an apoptotic reaction may also be induced by the preferential synthesis of apoptosis inducing proteins such as c-jun [20] or c-myc [22]. As shown in Table 1, several gene transcripts linked to apoptosis are present in higher levels in 18f-infected cells compared to clone 1 infected cells. Particularly intriguing are lack of induction of c-myc and down-regulation of c-jun in clone 1 infected cells. We cannot rule out the possibility, therefore, that apoptosis in 18f-infected cells may be induced via regulation of relevant proteins such as c-jun or c-myc.

Another interesting feature of the cp strains of HAV is that all apoptosis inducing cp strains are derived from persistently infected monkey kidney cells and induction of apoptosis (or cpe) is restricted to monkey kidney cells. Therefore, the nature of the host cell is clearly as important as the genetic makeup of the virus. It is interesting to note that a 14 base insertion is present in the IRES of cp strains HM175/18f as well as HM175/24a. It would be tempting to speculate that conformational changes brought about by this or other mutations result in a better inducer of 2'-5'A synthetase, a possibility that is currently under investigation.

Activation of RNase L resulting in rRNA cleavage is usually accompanied by inhibition of protein synthesis [6, 12, 30, 52, 69] and picornavirus growth [14, 53, 69]. We believe that the apparent lack of inhibition of host protein synthesis in 18f-infected cells is a result of asynchronous RNA degradation, which masks the effect of RNA degradation on protein synthesis. The other possibility is the absence of activation of dsRNA stimulated PKR, which may be lacking in these cells. However, several different mechanisms exist, through which viruses can disarm the PKR response [58, 59]. Further studies are required to assess the level of activity of this enzyme in virus-infected cells.

Recent studies using DNA arrays have revealed that genes involved in the interferon pathway (interferon response genes, ISGs) are the major targets of a diverse group of viruses [27]. A direct effect of interferon in inducing 2'-5'A synthetase during 18f or CBV infection is unlikely because we failed to detect

IFN mRNA or STAT1 phosphorylation in either uninfected or virus infected cells. These results are supported by previous findings that cell culture adapted HAV does not induce IFN in cultured cells [63]. Moreover, recent studies also have shown that a non-cytopathic cc strain of HAV down regulates dsRNA-induced transcription of β -IFN [8]. However, there are now several studies to show that ISGs can be regulated in the absence of IFN by viral dsRNA or viral proteins [6, 45, 64]. While many viruses have evolved mechanisms to disarm various facets of the IFN inducible antiviral response, the usurpation of the IFN response by the cp strain 18f to facilitate its spread is unique. The fact that only a few cell lines of primate kidney origin are susceptible to apoptosis in response to rapidly replicating HAV variants suggests that both cellular processes and genotypic changes in the viral genome are responsible for the establishment of a cp phenotype. In order to define the contributions of these two processes, it will be necessary to examine strain differences at the genetic level as they relate to substantive changes in viral protein expression/function, and to investigate the connection between viral and cellular events at the level of cellular protein expression.

In conclusion, rRNA degradation in combination with lower levels of cellular mRNAs such as β -actin, GAPDH and others could confer on the 18f virus a replicative advantage over the parental cc strain. Clearly, reduction in the levels of cellular mRNAs is advantageous to the virus, even if it leads to a small reduction rather than a dramatic shut-off of host protein synthesis.

Acknowledgments

We thank Dr. Darcy Hanes for help in preparing the anti-VP1 antiserum, Dr. Joseph E. LeClerc and Dr. Dan Levy for critically reading the manuscript, Dr. C.D. Atreya and Dr. Stephen Feinstone for helpful discussions, and Marcia Meltzer for help with the graphics.

References

1. Agol VI, Belov GA, Bienz K, Egger D, Kolesnikova M, Romanova L, Sladkova L, Tolskaya EA (2000) Competing death programs in poliovirus-infected cells: commitment switch in the middle of the infectious cycle. *J Virol* 74: 5534–5541
2. Anderson DA (1987) Cytopathology, plaque assay, and heat inactivation of hepatitis A virus strain HM175. *J Med Virol* 22: 35–44
3. Banerjee S, An S, Zhou A, Silverman RH, Makino S (2000) RNase-L-independent specific 28S rRNA cleavage in murine coronavirus-infected cells. *J Virol* 74: 8793–8802
4. Barco A, Feduchi E, Carrasco L (2000) Poliovirus protease 3C^{pro} kills cells by apoptosis. *Virology* 266: 352–360
5. Blank CA, Anderson DA, Beard M, Lemon SM (2000) Infection of polarized cultures of human intestinal epithelial cells with hepatitis A virus: vectorial release of progeny virions through apical cellular membranes. *J Virol* 74: 6476–6484
6. Bourgeade MF, Laurent-Winter C, Besancon F, Thang MN, Memet S (1993) Differential kinetics of polypeptide expression and different biological activities in

- the human fibroblast response to dsRNA or interferon treatment. *J Interferon Res* 13: 175–186
7. Brack K, Werner F, Dotzauer A, Vallbracht A (1998) A cytopathogenic, apoptosis inducing variant of hepatitis A virus. *J Virol* 72: 3370–3376
 8. Brack K, Berk I, Magulski T, Lederer J, Datzauer A, Vallbracht A (2002) Hepatitis A virus inhibits cellular antiviral defense mechanisms induced by double stranded RNA. *J Virol* 76: 11920–11930
 9. Brown EA, Zajac AJ, Lemon SM (1994) *In vitro* characterization of an internal ribosomal entry site (IRES) present within the 5' nontranslated region of the hepatitis A virus RNA: comparison with the IRES of encephalomyocarditis virus. *J Virol* 68: 1066–1074
 10. Carhty CM, Granville DJ, Watson KA, Anderson DR, Wilson JE, Yang D, Hunt DWC, McManus BM (1998) Caspase activation and specific cleavage of substrates after coxsackievirus B3-induced cytopathic effect in Hela cells. *J Virol* 72: 7669–7675
 11. Castelli JC, Hassel BA, Wood KA, Li XL, Amemiya K, Dalakas MC, Torrence PF, Youle RJ (1997) A study of the interferon antiviral mechanism: Apoptosis activation by the 2-5A system. *J Exp Med* 186: 967–972
 12. Castelli JC, Hassel BA, Maran A, Paranjape J, Hewitt JA, Li X-L, Hsu Y-T, Silverman RH, Youle RJ (1998) The role of 2'-5' oligoadenylate-activated ribonuclease L in apoptosis. *Cell Death Differ* 5: 313–320
 13. Chang KH, Brown EA, Lemon SM (1993) Cell type-specific proteins which interact with the 5' nontranslated region of hepatitis A virus RNA. *J Virol* 67: 6716–6725
 14. Chebath J, Benech P, Revel M, Vigneron M (1987) Constitutive expression of (2'-5') oligo A synthetase confers resistance to picornavirus infection. *Nature* 330: 587–588
 15. Cho MW, Ehrenfeld E (1991) Rapid completion of the replication cycle of hepatitis A virus subsequent to reversal of guanidine inhibition. *Virology* 180: 770–780
 16. Chomczynski P, Mackey K (1992) One-hour downward capillary blotting of RNA at neutral pH. *Anal Biochem* 221: 303–305
 17. Cliver DO (1985) Vehicular transmission of hepatitis A. *Publ Health Rev* 13: 235–292
 18. Cohen JL, Rosenblum B, Ticehurst JR, Doemer R, Feinstone SM, Purcell RH (1987) Complete nucleotide sequence of an attenuated hepatitis A virus: comparison with wild-type virus. *Proc Natl Acad Sci USA* 84: 2497–2501
 19. Cohrs RJ, Goswami BB, Sharma OK (1988) Occurance of 2-5A and RNA degradation in chick oviduct during rapid estrogen withdrawal. *Biochemistry* 27: 3246–3252
 20. Colotta F, Polentarutti N, Sironi M, Mantovani A (1992) Expression and involvement of c-fos and c-jun protooncogenes in programmed cell death induced by growth factor deprivation in lymphoid cell lines. *J Biol Chem* 267: 18278–18283
 21. Cromeans T, Sobsey MD, Fields HA (1987) Development of plaque assay for a cytopathic, rapidly replicating isolate of hepatitis A virus. *J Med Virol* 22: 45–56
 22. Dang CV (1999) C-Myc target genes involved in cell growth, apoptosis, and metabolism. *Mol Cell Biol* 19: 1–11
 23. De Chastonay J, Siegl G (1987) Replicative events in hepatitis A virus infected MRC-5 cells. *Virology* 157: 268–275
 24. Diaz-Guerra M, Rivas C, Esteban M (1997) Activation of the interferon-inducible enzyme Rnase L causes apoptosis of animal cells. *Virology* 236: 354–363
 25. Divizia M, Ruggeri F, Hentschel J, Flemig B, Pana A, Perez-bercoff R (1986) Preliminary characterization of a fast-growing strain of human hepatitis A virus. *Microbiologica* 9: 269–278

26. Emerson SU, Huang YK, Purcell RH (1993) 2B and 2C mutations are essential but mutations throughout the genome of HAV contributes to adaptation to cell culture. *Virology* 194: 475–480
27. Fruh K, Simmen K, Mattias Luukkonen BG, Bell YC, Ghazal P (2001) Virogenomics: a novel approach to antiviral drug discovery. *Drug Discover Today* 6: 621–627
28. Funkhouser AW, Schultz DE, Lemon SM, Purcell RH, Emerson SE (1999) Hepatitis A virus translation is rate limiting for virus replication in MRC-5 cells. *Virology* 254: 268–278
29. Gosert R, Egger D, Bienz K (2000) A cytopathic and a cell culture adapted hepatitis A virus strain differ in cell killing but not in intracellular membrane rearrangement. *Virology* 266: 157–169
30. Goswami BB, Sharma OK (1984) Degradation of rRNA in interferon-treated vaccinia virus infected cells. *J Biol Chem* 259: 1371–1374
31. Goswami BB, Kulka M, Ngo D, Istafanos P, Cebula TA (2002) A polymerase chain reaction-based method for the detection of hepatitis A virus in produce and shellfish. *J Food Prot* 65: 393–402
32. Graff J, Ehrenfeld E (1998) Coding sequences enhance internal initiation of translation by hepatitis A virus RNA *in vitro*. *J Virol* 72: 3571–3577
33. Gust ID (1988) Prevention and control of hepatitis A. In: AJ Zuckerman (Ed), *Viral hepatitis and liver disease*. Alan R Liss, New York, pp 77–80
34. Harmon SA, Emerson SU, Huang YK, Summers DF, Ehrenfeld E (1995) Hepatitis A viruses with deletions in the 2A gene are infectious in cultured cells and marmosets. *J Virol* 69: 5576–5581
35. Iordanov M, Paranjape JM, Zhou A, Wong J, Williams BRG, Meurs EF, Silverman RH, Magun BE (2000) Activation of P38 mitogen-activated protein kinase and c-jun NH2-terminal kinase by double-stranded RNA and encephalomyocarditis virus: involvement of RNase L, protein kinase R, and alternative pathways. *Mol Cell Biol* 20: 617–627
36. Iordanov M, Wong J, Bell JC, Magun BE (2001) Activation of NF- κ B by double-stranded RNA (dsRNA) in the absence of protein kinase R and RNase L demonstrates the existence of two separate dsRNA triggered antiviral programs. *Mol Cell Biol* 21: 61–72
37. Jecht M, Probst C, Gauss-Muller V (1998) Membrane permeability induced by hepatitis A virus proteins 2B and 2BC and proteolytic processing of HAV 2BC. *Virology* 252: 218–227
38. Jia X-Y, Tesar M, Summers DF, Ehrenfeld E (1996) Replication of hepatitis A viruses with chimeric 5' nontranslated regions. *J Virol* 70: 2861–2868
39. Kerekatte V, Keiper BD, Badorff C, Cai A, Knowlton KU, Rhoads RE (1999) Cleavage of poly (A)-binding protein by coxsackievirus 2A protease *in vitro* and *in vivo*: another mechanism for host protein synthesis shutoff? *J Virol* 73: 709–717
40. Kusov Y, Weitz M, Dollenmeier G, Gauss-Muller V, Seigl G (1996) RNA-protein interaction at the 3' end of the hepatitis A virus RNA. *J Virol* 70: 1890–1897
41. Lai MMC (1998) Cellular factors in the transcription and replication of viral genomes: a parallel to DNA-dependent RNA transcription. *Virology* 244: 1–12
42. Lemon SM, Murphy PC, Shields PA, Ping L-H, Feinstone SM, Cromeans T, Jansen RW (1991) Antigenic and genetic variation in cytopathic hepatitis A virus variants arising during persistent infection: evidence for genetic recombination. *J Virol* 65: 2056–2065
43. Martin A, Benichou D, Chao SF, Cohen LM, Lemon SM (1999) Maturation of the hepatitis A virus capsid protein VP1 is not dependent on processing by the 3C^{pro} proteinase. *J Virol* 73: 6220–6227

44. Martinand C, Salehzada T, Silhol M, Lebleu B, Bisbal C (1998) The RNase L inhibitor (RLI) is induced by double-stranded RNA. *J Interferon Cytokine Res* 18: 1031–1038
45. Memet S, Besancon F, Bourgeade MF, Thang MN (1991) Direct induction of interferon-gamma- and interferon-alpha/beta inducible genes by double-stranded RNA. *J Interferon Res* 11: 131–141
46. Naganuma A, Nozaki A, Tanaka T, Sugiyama K, Takagi H, Mori M, Shimotohno K, Kato K (2000) Activation of the interferon inducible 2'-5'-oligoadenylate synthetase gene by hepatitis C virus coat protein. *J Virol* 74: 8744–8750
47. Nasser AM, Metcalf TG (1987) Production of cytopathology in FrhK4 cells by BS-C-1 passaged hepatitis A virus. *Appl Environ Microbiol* 53: 2967–2971
48. Nüesch JPF, De Chastonay J, Siegl G (1989) Detection of defective genomes in hepatitis A virus particles present in clinical specimens. *J Gen Virol* 70: 3475–3480
49. Pietiäinen V, Huttunen P, Hyypiä T (2000) Effects of echovirus 1 infection on cellular gene expression. *Virology* 276: 243–250
50. Pisani G, Beneduce F, Gauss-Muller V, Morace G (1995) Recombinant expression of hepatitis A virus protein 3A: interaction with membranes. *Biochem Biophys Res Commun* 211: 627–638
51. Roulston A, Marcellus RC, Branton PE (1999) Viruses and Apoptosis. *Annu Rev Microbiol* 53: 577–628
52. Rusch L, Zhou A, Silverman RH (2000) Caspase-dependent apoptosis by 2'-5'-oligoadenylate activation of RNase L is enhanced by IFN- β . *J Interferon Cytokine Res* 20: 1091–1100
53. Rysiecki G, Gewert DR, Williams BRG (1989) Constitutive expression of a 2',5'-oligoadenylate synthetase cDNA results in increased antiviral activity and growth suppression. *J Interferon Res* 9: 649–657
54. Schultheiss T, Kusov Y, Gauss-Muller V (1994) Proteinase 3C of hepatitis A virus (HAV) cleaves the HAV polyprotein P2–P3 at all sites including VP1/2A and 2A/2B. *Virology* 198: 275–281
55. Schultz D, Hardin CC, Lemon SM (1996) Specific interaction of glyceraldehydes 3-phosphate dehydrogenase with the 5' nontranslated RNA of hepatitis A virus. *J Biol Chem* 271: 14134–14142
56. Seipelt J, Guarné A, Bergmann E, James M, Sommergruber W, Fita I, Skern T (1999) The structures of picornaviral proteinases. *Virus Res* 62: 159–168
57. Siegl G, Weitz M, Kronauer G (1984) Stability of hepatitis A virus. *Intervirology* 22: 218–226
58. Sen G (2001) Viruses and interferons. *Annu Rev Microbiol* 55: 255–281
59. Stark GR, Kerr IM, Williams BRG, Silverman RH, Schreiber RD (1998) How cells respond to Interferons. *Annu Rev Biochem* 67: 227–264
60. Tolskaya EA, Romanova LI, Kolesnikova MS, Ivannikova TA, Smirnova EA, Raikhlin NT, Agol VI (1995) Apoptosis-inducing and apoptosis-preventing functions of poliovirus. *J Virol* 69: 1181–1189
61. Tsunoda I, Kurtz CI, Fujinami RS (1997) Apoptosis in acute and chronic central nervous system disease induced by Theiler's murine encephalomyelitis virus. *Virology* 228: 388–393
62. Venuti A, Di Russo C, del Grosso N, Patti AM, Ruggeri F, De Stasio PR, Martiniello MG, Pagnotti P, Degener AM, Midulla M (1986) Isolation and molecular cloning of a fast growing strain of human hepatitis A virus from its double stranded replicative form. *J Virol* 56: 579–588
63. Vallbracht A, Gabriel P, Zahn J, Flehmig B (1985) Hepatitis A virus infection and the interferon system. *J Infect Dis* 152: 211–213

64. Wathelet MG, Clauss IM, Content J, Huez GA (1988) Regulation of two interferon inducible human genes by interferon, poly(rI):poly(rC) and viruses. *Eur J Biochem* 174: 323–329
65. Weitz M, Baroudy BM, Maloy WL, Ticehurst JR, Purcell RH (1986) Detection of a genome-linked protein (VPg) of hepatitis A Virus and its comparison with other picornaviral VPgs. *J Virol* 60: 124–130
66. Whetter LE, Day SP, Elroy-Stein O, Brown EA, Lemon SM (1994) Low efficiency of the 5' nontranslated region of hepatitis A RNA in directing cap-independent translation in permissive monkey kidney cells. *J Virol* 68: 5253–5263
67. Yi M, Schultz DE, Lemon SM (2000) Functional significance of the interaction of hepatitis A virus RNA with glyceraldehydes 3-phosphate dehydrogenase (GAPDH): opposing effects of GAPDH and polypyrimidine tract binding protein on internal ribosome entry site function. *J Virol* 74: 6459–6468
68. Zhang H, Chao S-H, Ping L-H, Grace K, Clarke B, Lemon SM (1995) An infectious cDNA clone of a cytopathic hepatitis A virus: genomic regions associated with rapid replication and cytopathic effect. *Virology* 212: 686–697
69. Zhou A, Paranjape JM, Hassel BA, Nie H, Shah S, Galinsky B, Silverman RH (1998) Impact of RNase L overexpression on viral and cellular growth and death. *J Interferon Cytokine Res* 18: 953–961

Author's address: Biswendu B. Goswami, Ph.D., Division of Molecular Biology, HFS-025, Center for Food Safety and Applied Nutrition, Food and Drug Administration, 8301 Muirkirk Road, Laurel, MD 20708, U.S.A.; e-mail: bgoswami@cfsan.fda.gov